ABSOLUTE DIMENSIONS OF THE F-TYPE ECLIPSING BINARY STAR VZ CEPHEI

Guillermo Torres[1], and Claud H. Sandberg Lacy[2]
Draft version October 28, 2008

ABSTRACT

We present new V-band differential photometry and radial-velocity measurements of the unevolved 1.18-day period F+G-type double-lined eclipsing binary VZ Cep. We determine accurate values for the absolute masses, radii, and effective temperatures as follows: $M_A = 1.402 \pm 0.015$ M$_\odot$, $R_A = 1.534 \pm 0.012$ R$_\odot$, $T_{eff} = 6690 \pm 160$ K for the primary, and $M_B = 1.1077 \pm 0.0083$ M$_\odot$, $R_B = 1.042 \pm 0.039$ R$_\odot$, $T_{eff} = 5720 \pm 120$ K for the secondary. A comparison with current stellar evolution models suggests an age of 1.4 Gyr for a metallicity near solar. The temperature difference between the stars, which is much better determined than the absolute values, is found to be ~250 K larger than predicted by theory. If all of this discrepancy is attributed to the secondary (which would then be too cool compared to models), the effect would be consistent with similar differences found for other low-mass stars, generally believed to be associated with chromospheric activity. However, the radius of VZ Cep B (which unlike the primary, still has a thin convective envelope) appears normal, whereas in other stars affected by activity the radius is systematically larger than predicted. Thus, VZ Cep poses a challenge not only to standard theory but to our understanding of the discrepancies in other low-mass systems as well.

Subject headings: binaries: eclipsing — stars: evolution — stars: fundamental parameters — stars: individual (VZ Cep)

1. INTRODUCTION

VZ Cephei (also known as BD +70 1199 and GSC 04470-01334; $\alpha = 21^h 50^m 11^s.14$, $\delta = +71° 26' 38''.3$, J2000.0; $V = 9.72$) was discovered photographically as a variable star by Gengler et al. (1928), who classified it to be of type "Is?", a rapid irregular variable. Cannon (1934) made the first spectral type assignment as G0. Its discovery as an eclipsing binary is due to Rössiger (1978), who determined a period of 1.18336 days and showed it to have unequal minima. The system was included by Lacy (1992, 2002a) in his photometric surveys of eclipsing binary stars. Because of its relatively late spectral class, Popper (1996) had it as a target in his program to search for late-type (F–K) eclipsing binary stars. He concluded on the basis of 4 spectrograms that both stellar components were likely hotter than G0. No determinations have been made of the physical properties of the stars, and the system has generally been neglected except for measurements of the times of eclipse made by a number of investigators since 1994.

We began our investigation for the same reason Popper did: to test theoretical predictions of the properties of low-mass stars. We and other authors have previously found that in some of these binary systems the absolute properties are not well described by standard stellar evolution theory (see, e.g., Popper 1997; Clausen et al. 1999; Ribas 2006; Torres et al. 2006). We find below that VZ Cep also shows some anomalies compared to standard models, even though its components are both more massive than the Sun.

2. ECLIPSE EPHEMERIS

Photometric times of minimum light of VZ Cep available from the literature are collected in Table 1. Eclipse ephemerides determined by weighted least squares separately from the 15 primary minima and the 13 secondary minima gave the same period within the errors. A joint fit of all the measurements was then performed enforcing a common period but allowing the primary and secondary epochs to be free parameters. Scale factors for the internal errors were determined by iterations separately for the two types of measurements in order to achieve reduced χ^2 values near unity. This solution resulted in a phase difference between the two epochs of $\Delta\phi = 0.50033 \pm 0.00022$, not significantly different from 0.5. For our final ephemeris we imposed a circular orbit, and obtained

Min I (HJD) $= 2,452,277.324478(59) + 1.183363762(84) \cdot E$.

The uncertainties of the fitted quantities in terms of the least significant digit are shown in parentheses. The final scale factors for the published internal errors were similar to those in the previous fit, and were 1.38 for the primary and 2.42 for the secondary. We adopt this ephemeris for the spectroscopic and photometric analyses below.

3. SPECTROSCOPIC OBSERVATIONS AND ORBIT

VZ Cep was placed on the observing list at the Harvard-Smithsonian Center for Astrophysics (CfA) in 2003 January, and was observed until 2007 June with an echelle spectrograph on the 1.5-m Tillinghast reflector at the F. L. Whipple Observatory (Mount Hopkins, AZ). A single echelle order 45 Å wide centered at 5188.5 Å was recorded with an intensified Reticon photon-counting diode array, at a resolving power of $\Delta\lambda/\lambda \approx 35,000$. The strongest lines in this window are those of the Mg I b triplet. A total of 39 spectra were obtained with signal-to-noise ratios ranging from 19 to 47 per resolution element of 8.5 km s^{-1}.

[1] Harvard-Smithsonian Center for Astrophysics, 60 Garden Street, Cambridge, MA 02138, e-mail: gtorres@cfa.harvard.edu
[2] Department of Physics, University of Arkansas, Fayetteville, AR 72701, e-mail: clacy@uark.edu

Radial velocities were measured with the two-dimensional cross-correlation technique TODCOR (Zucker & Mazeh 1994). Templates for the primary and secondary were selected from a large library of synthetic spectra based on model atmospheres by R. L. Kurucz[3] (see also Nordström et al. 1994; Latham et al. 2002). These calculated spectra cover a wide range of effective temperatures (T_{eff}), rotational broadenings ($v \sin i$ when seen in projection), surface gravities ($\log g$), and metallicities. Solar metallicity was assumed throughout, along with initial values of $\log g = 4.5$ for both components. The temperatures and rotational velocities for the templates were determined by running extensive grids of two-dimensional cross-correlations and seeking the best correlation value averaged over all exposures, as described in more detail by Torres et al. (2002). The secondary component in VZ Cep is some 5 times fainter than the primary, and we were unable to determine its temperature independently. We therefore adopted the results from other estimates described below, and chose the nearest value in our library, which is 5750 K. Due to the narrow wavelength range of our spectra the derived temperatures are strongly correlated with the assumed surface gravities. The secondary $\log g$ presented in § 5 is very close to the value we assumed, but the primary $\log g$ is intermediate between 4.0 and 4.5, so we repeated the calculations above using the lower value, and interpolated. The results for the primary are $T_{eff} = 6690 \pm 150$ K and $v \sin i = 57 \pm 3$ km s^{-1}, and for the secondary we obtain $v \sin i = 50 \pm 10$ km s^{-1}. Radial velocities were derived with template parameters near these values. The stability of the zero-point of the CfA velocity system was monitored by means of exposures of the dusk and dawn sky, and small run-to-run corrections were applied in the manner described by Latham (1992).

Possible systematics in the radial velocities that may result from residual line blending in our narrow spectral window, or from shifts of the spectral lines in and out of this window as a function of orbital phase, were investigated by performing numerical simulations as described by Torres et al. (1997, 2000). Briefly, we generated artificial composite spectra by adding together copies of the two templates with scale factors in accordance with the light ratio reported below, and with Doppler shifts for each star appropriate for each actual time of observation, computed from a preliminary orbital solution. These simulated spectra were then processed with TODCOR in the same manner as the real spectra, and the input and output velocities were compared. Experience has shown that the magnitude of these effects is difficult to predict, and must be studied on a case-by-case basis. Corrections were determined for VZ Cep based on these simulations and were applied to the raw velocities. The corrections for the primary star are small (under 1 km s^{-1}), but for the secondary they are as large as 11 km s^{-1}, and as expected they vary systematically with orbital phase or radial velocity (see Figure 1). Similarly large corrections have been found occasionally for other systems using the same instrumentation (e.g., AD Boo, GX Gem; Clausen et al. 2008; Lacy et al. 2008). The impact of these corrections is quite significant for VZ Cep: the minimum masses increase by 4% for the primary and
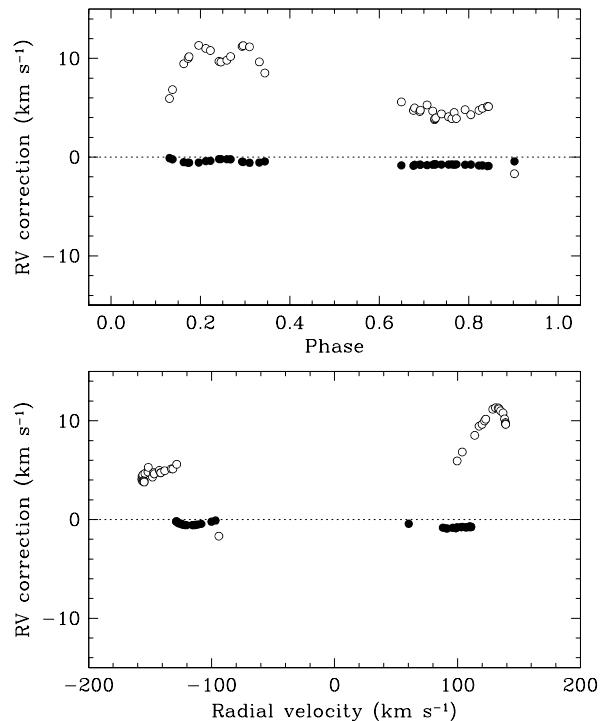

Fig. 1.— Corrections for systematics in the radial-velocity measurements for VZ Cep as a function of orbital phase and radial velocity (see text). Filled circles correspond to the primary and open circles to the secondary.

1.9% for the secondary, and the mass ratio decreases by 2.1%. The final velocities in the heliocentric frame, including the corrections for systematics, are listed in Table 2 and have typical uncertainties of 1.3 km s^{-1} for the primary and 3.8 km s^{-1} for the fainter secondary.

Preliminary single-lined orbital solutions using the primary and secondary velocities separately indicated a zero-point difference between the two data sets (i.e., a difference in the systemic velocity γ), which is often seen by many investigators in cases where there is a slight mismatch between the templates used for the cross-correlations and the spectra of the real stars (see, e.g., Popper 2000; Griffin et al. 2000). Numerous tests with other templates did not remove the offset.[4] This most likely arises in our case because of stellar parameters (particularly the rotation) that fall in between the template parameters available in our library of synthetic spectra, which come in rather coarse steps of 10 km s^{-1} at the high rotation rates of VZ Cep. We therefore included this velocity offset as an additional free parameter in the double-lined orbital fit, and we verified that when doing so the velocity semi-amplitudes (which determine the masses) are insensitive to the exact template parameters within reasonable limits, and are essentially identical to those resulting from separate single-lined solutions. Our final orbital fit is presented in Table 3. No indication of eccentricity was found, as expected for such a short period, so only a circular orbit was considered in the following. A graphical representation of the observations and our best fit, along with the residuals, is shown

[4] As a further test, solutions without applying the corrections for systematics described in the preceding paragraph gave an offset more than twice as large.
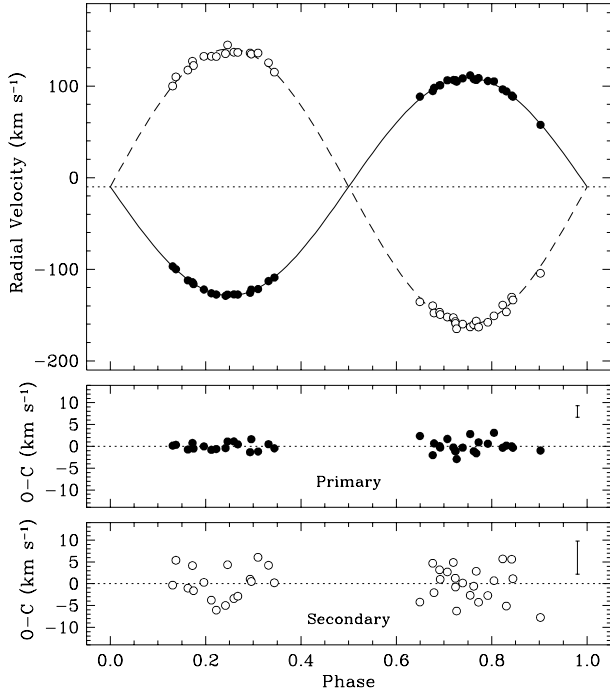
FIG. 2.— Radial-velocity measurements for VZ Cep (including the corrections for systematics described in the text) along with our spectroscopic orbital solution. Filled circles correspond to the primary, and the dotted line represents the center-of-mass velocity. Error bars are smaller than the size of the points. The $O - C$ residuals are shown on an expanded scale in the bottom panels, where typical error bars are indicated in the upper right corner.

in Figure 2.

The light ratio between the primary and secondary was determined from our spectra following Zucker & Mazeh (1994), accounting for the difference in line blocking between the primary and the much cooler secondary. After corrections for systematics analogous to those described above, we obtained $L_B/L_A = 0.19 \pm 0.02$ at the mean wavelength of our observations. A further adjustment to the visual band taking into account the temperature difference between VZ Cep A and B was determined from synthetic spectra integrated over the V passband and the spectral window of our observations, and resulted in $(L_B/L_A)_V = 0.22 \pm 0.02$.

4. PHOTOMETRIC OBSERVATIONS AND ANALYSIS

Differential photometry of VZ Cep was obtained at the URSA Observatory on the University of Arkansas campus at Fayetteville, AR. The URSA Observatory sits atop Kimpel Hall and consists of a Meade f/6.3, 10-inch Schmidt-Cassegrain telescope with a Santa Barbara Instruments Group ST8EN CCD camera inside a Technical Innovations RoboDome, all controlled by a Macintosh G4 computer in an adjacent control room inside the building. The field of view is $20' \times 30'$. Images of VZ Cep ($V \approx 9.7$) and the two comparison stars GSC 04470-01497 ($V \approx 9.9$) and GSC 04470-01622 ($V \approx 11.2$), both of which are within 6′ of the target, were taken with typical integration times of 60 seconds through a Bessell V filter. With an overhead of about 30 seconds to download the images from the camera, the observing cadence was typically 90 seconds per image. A "virtual measuring engine" application written by Lacy was used to determine the brightness of the variable and comparison
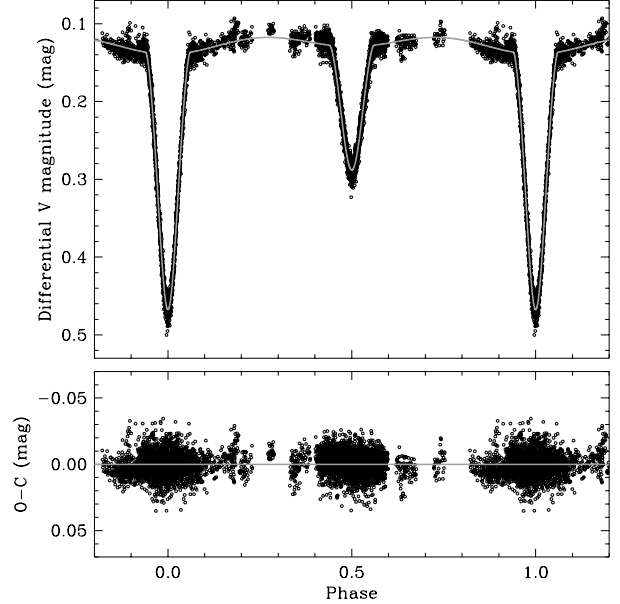

FIG. 3.— V-band photometric measurements for VZ Cep, along with our best constrained model described in the text. $O - C$ residuals are shown at the bottom.

stars, to subtract off the sky brightness, and to correct for differences in airmass. A total of 5473 images were gathered between 2001 March 5 and 2003 September 7. Differential magnitudes were formed between the variable star and the magnitude corresponding to the sum of the fluxes of the two comparison stars. These are listed in Table 4, and shown graphically in Figure 3 along with our modeling described below. Expanded views of the primary and secondary eclipse are given in Figure 4 and Figure 5. The typical precision of these measurements is about 0.007 mag, which is comparable to that expected from photon statistics ($\sim$0.006 mag). The comparison stars are not known to be variable. The mean magnitude difference between the two was constant with a standard deviation of 0.0095 mag over 67 nights, which is what would be expected for individual magnitudes with a typical error of 0.007 mag. A Lomb-Scargle periodogram analysis of the individual differences was performed to search for periodic signals in either star, but none were detected.

We have previously found (Lacy et al. 2008) that the URSA photometry is significantly improved by removal of small nightly zero-point variations. Thus 67 nightly corrections were made to the original magnitudes based on a preliminary photometric orbital fit. This procedure reduced the residual standard deviation by about 15%, a small but significant amount. Examination of these offsets, which are typically smaller than 0.01 mag, revealed no detectable pattern as a function of orbital phase. Such a pattern might be expected, for instance, if there were perturbations in the light curve due to spots on either star (assuming synchronous rotation). We thus consider the nightly offsets to be instrumental in nature.

The corrected photometry was fitted with the NDE model (Etzel 1981; Popper & Etzel 1981), with all observations being assigned equal weight. In this model the stars are represented as biaxial ellipsoids, and despite the relatively large radius of the primary of VZ Cep
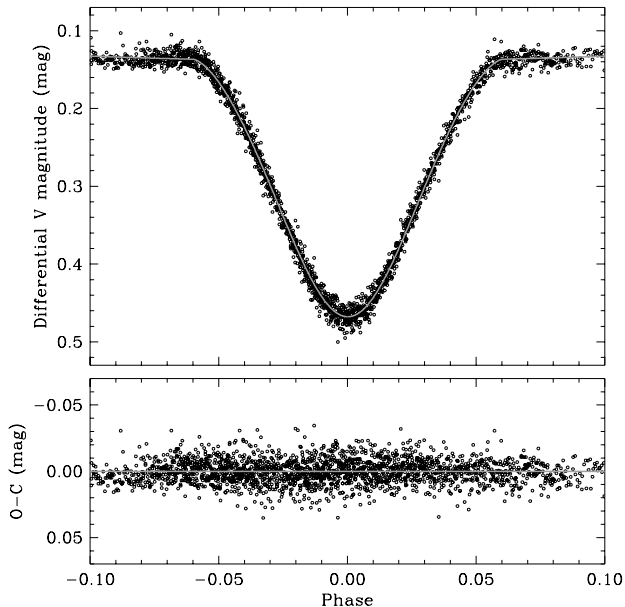
FIG. 4.— Enlarged view of Figure 3 showing the V-band pho-
tometry for VZ Cep around the primary minimum. $O-C$ residuals
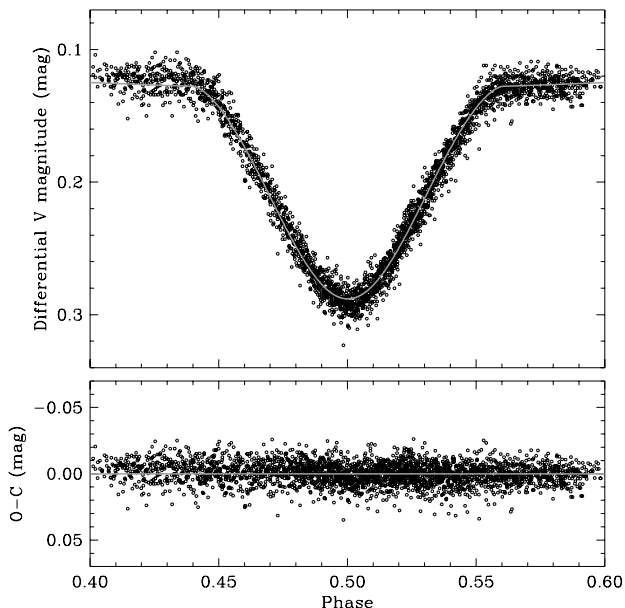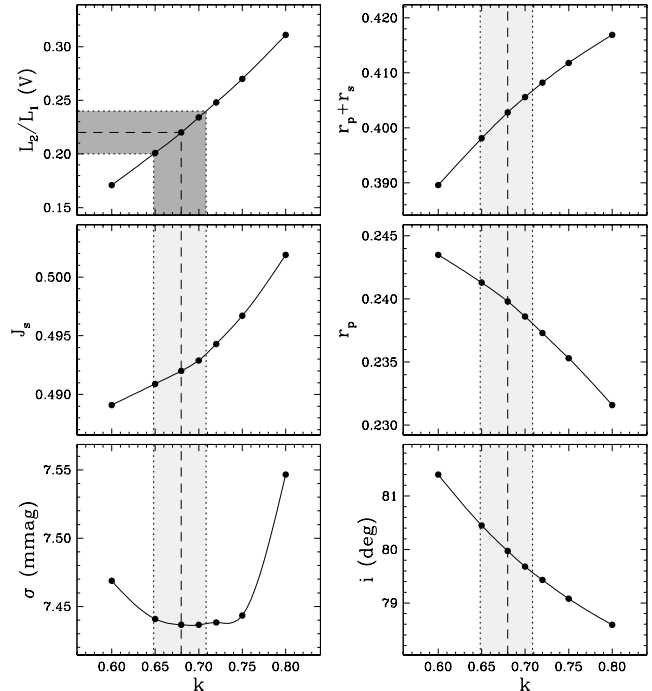are shown at the bottom.

FIG. 6.— Application of the constraint given by the spectro-
scopic brightness ratio to the light curve fits of VZ Cep. Grids of
solutions for fixed values of k are shown for several key parame-
ters, along with the corresponding rms residual of the fit (σ). The
spectroscopic value $(L_B/L_A)_V = 0.22 \pm 0.02$ is applied in the top
left panel to determine k, and all other quantities are interpolated
to the same value.

(cooler) star relative to the primary, the sum of relative
radii $r_A + r_B$, the ratio of radii r_B/r_A, the orbital in-
clination i, the limb-darkening coefficients u_A and u_B, a
phase offset, and the magnitude at quadrature. The fol-
lowing quantities were kept fixed: the orbital eccentric-
ity $e = 0$, the mass ratio from the spectroscopic solution
$q \equiv M_B/M_A = 0.7900$, and the gravity brightening expo-
nents $y_A = 0.25$ and $y_B = 0.36$, set by the temperatures
and surface gravities following Claret (1998). The uncer-
tainties of the adjustable parameters were estimated with
a Monte Carlo technique in which we generated 500 syn-
thetic light curves, solved for the parameters, and calcu-
lated the standard error of each parameter. This process
yielded uncertainty estimates accurate to two significant
digits, which is sufficient for our purposes. These "Un-
constrained" results are given in Table 5. Tests allowing
for non-zero eccentricity and third light gave statistically
insignificant values for those quantities.

The V-band light ratio $(L_B/L_A)_V$ from this fit is
consistent with our spectroscopic value from §3, but
formally less precise. In similar systems with partial
eclipses, the *accuracy* of the parameters (more than their
precision) is sometimes compromised because of strong
correlations among variables and the relatively flat bot-
tom of the χ^2 surface in the least-squares problem (see,
e.g., Andersen 1991). In such systems it is often the case
that more accurate results are obtained by applying the
spectroscopic light ratio as an external constraint. We
have done this here by first computing a grid of solutions
for a range of fixed values of k. We then interpolated in
the smooth relation obtained between the light ratio and
k to our value of $(L_B/L_A)_V = 0.22 \pm 0.02$, and derived

FIG. 5.— Enlarged view of Figure 3 showing the V-band photom-
etry for VZ Cep around the secondary minimum. $O-C$ residuals
are shown at the bottom.

relative to the separation (see below), its ellipticity of
0.016, as defined by Etzel (1981), is still well below the
maximum tolerance of 0.04 (Popper & Etzel 1981), and
thus the model is expected to be adequate for this case.
We return to this below. We used the JKTEBOP imple-
mentation of Southworth et al. (2007) with a linear limb-
darkening law, consistent with our findings (Lacy et al.
2005, 2008) that with the amount and precision of our
data, non-linear limb-darkening laws do not improve the
accuracy of the fits significantly. The following quan-
tities were allowed to vary in this unconstrained solu-
tion: the central surface brightness J_B of the secondary

$k = 0.680\pm0.030$. Interpolations of all other quantities to this value of k were then carried out. This is illustrated in Figure 6 for some of the key light-curve parameters. Note that σ, the rms residual of the fit, changes very little for k between 0.65 and 0.75, demonstrating that the radius ratio cannot be determined accurately from photometry alone without an external constraint. The results for the light curve parameters from this constrained fit are listed in Table 5, and are adopted for further use. The uncertainties have been propagated directly from the error in the spectroscopic light ratio (see Figure 6), and include also a contribution from the statistical uncertainties derived from a separate solution in which k was fixed at the best-fit value and all other parameters were left free.

The fitted linear limb-darkening coefficients from this constrained solution tend to be somewhat smaller than predicted by theory. We find, for example, marginal differences of 0.10 ($\sim1.3\sigma$) for both stars compared to the calculations by van Hamme (1993), and more significant differences of 0.19 (2.5σ) compared to the coefficients by Claret (2000). These differences are similar in magnitude (and in this particular case, of the same sign) as those reported, e.g., by Southworth (2008), and may be due to shortcomings in the theoretical model atmospheres although observational errors cannot be ruled out. For further comparisons between theory and observations the reader is referred to the recent work of Claret (2008). Adopting coefficients from the tables by Claret (2000) leads to values of the relative radii that are larger by 1.1% for the primary and 1.7% for the secondary (1.6σ and 0.5σ, respectively).

As a test of the reliability of the geometric parameters, we carried out solutions with two other light-curve modeling programs that are more sophisticated than the one we have used. One is the WINK program (Wood 1972), which adopts a better approximation to the stellar shapes as triaxial ellipsoids, rather than the simpler biaxial ellipsoids in EBOP, and includes a more detailed treatment of reflection effects. The version we used has been modified and extended as described by Vaz (1984, 1986), Vaz (1985), and Nordlund & Vaz (1990). The other program is the Wilson-Devinney code (WD; Wilson & Devinney 1971; Wilson 1979, 1990, 1993; van Hamme 2007) in its most recent (2007) release, which uses Roche geometry. Light curve solutions with these two codes were performed for a fixed value of $k = 0.680$ (as closely as allowed by the different input quantities) to permit a direct comparison with our constrained JKTEBOP fit, and with the same limb-darkening law and coefficients as used earlier. The WINK fit delivered marginally smaller relative radii that differ from our JKTEBOP results by $\Delta r_A = -0.0009$ and $\Delta r_B = -0.0005$ (i.e., less than 0.4%), and an inclination angle that was only $\Delta i = +0\overset{\circ}{.}03$ larger. The WD fit gave $\Delta r_A = -0.0008$, $\Delta r_B = -0.0005$, and $\Delta i = +0\overset{\circ}{.}22$. These results are thus not significantly different from those of the simpler model we have used, as expected from the relatively small ellipticity of the stars mentioned earlier.

The individual temperatures were determined from the central surface brightness parameter J_B slightly adjusted for limb darkening to correspond to the disk average (see, e.g., Lacy et al. 1987), the absolute visual flux scale of Popper (1980), and an estimate of the mean system temperature used as the initial value for

the primary. The latter was then improved by iteration until convergence. The mean system temperature is based on accurate Strömgren photometry for VZ Cep reported by Lacy (2002a). Interstellar reddening was estimated using the calibration of Perry & Johnston (1982) and the method of Crawford (1975), which resulted in $E(b - y) = 0.032 \pm 0.007$ and an intrinsic color index of $(b - y)_0 = 0.286 \pm 0.007$. The calibration by Holmberg et al. (2007) was then used to derive a mean system temperature of 6500 ± 150 K, assuming solar metallicity. The individual temperatures derived in this way are 6690 ± 160 K and 5720 ± 120 K for the primary and secondary, respectively, which correspond to spectral types of approximately F3 and G4 (Gray 1992, p. 430). The primary $T_{\rm eff}$ is identical to our spectroscopic estimate in § 3. The temperature difference based the light curve is of course better determined than the absolute values: $\Delta T_{\rm eff} = 970 \pm 35$ K. Use of a different color/temperature calibration for inferring the mean system temperature, such as that by Alonso et al. (1996), yields results only ~30 K hotter.

5. ABSOLUTE DIMENSIONS AND PHYSICAL PROPERTIES

The spectroscopic and photometric solutions above lead to the masses and radii given in Table 6. Also included are the predicted projected rotational velocities, calculated under the assumption of synchronism with the orbital motion. The secondary value is consistent with our measured $v \sin i$ from § 3, but the expected value of $64.6 \pm 0.5 \; {\rm km \, s^{-1}}$ for the primary seems somewhat larger than our spectroscopic estimate of $v \sin i = 57\pm3 \; {\rm km \, s^{-1}}$. At face value this would indicate sub-synchronous rotation of that component, which is unexpected in a short-period binary such as VZ Cep. Since the primary star dominates the light of the system, we investigated the possibility that there might be a photometric signal produced, for instance, by rotational modulation from surface features on that component. For this we examined the residuals from our adopted light curve solution. A Lomb-Scargle power spectrum did not indicate any significant periodicities within a factor of two of the orbital frequency, although the primary star is likely to be too hot for spots to be important (see § 7).

There are no measurements of the chemical abundance of VZ Cep. Our own spectroscopy is inadequate for this, and the combined-light Strömgren indices along with the calibration by Holmberg et al. (2007) indicate [Fe/H] $= +0.06 \pm 0.09$, in which the uncertainties include photometric errors as well as the scatter of the calibration. The *Hipparcos* catalog (Perryman et al. 1997) has no entry for VZ Cep and no trigonometric parallax is available. From its radiative properties as measured here we find the distance to the system to be 215 ± 10 pc (similar distances are obtained separately for each component, indicating the consistency of the measured properties).

Discrepancies described in the next section between our effective temperature estimates and the $T_{\rm eff}$ values predicted by stellar evolution models prompted us to attempt a deconvolution of the combined-light photometry of VZ Cep, as a check on both the color excess and the temperature difference between the components. We used tables of standard Strömgren indices by Crawford (1975) and Olsen (1984), and synthesized binary stars for a range of primary indices and a fixed

V-band light ratio given by our spectroscopic estimate of $(L_{\rm B}/L_{\rm A})_V = 0.22 \pm 0.02$. We explored a wide range of $E(b-y)$ values. At each reddening we determined the intrinsic indices for the primary and secondary that provide the best match to the system values of $b-y$, m_1, c_1, and β as measured by Lacy (2002a), in the χ^2 sense. We found the best agreement for $E(b-y) = 0.032$, in excellent accord with our earlier determination based on the combined light. The measured $b-y$, c_1, and β indices are reproduced to well within their uncertainties, and m_1 is within 1.8σ. Making use of the same color/temperature calibration by Holmberg et al. (2007) invoked earlier, the intrinsic indices for each star from this photometric deconvolution yield temperatures of 6670 K and 5690 K, once again in very good agreement with the light curve results. The temperature difference from this exercise is $\Delta T_{\rm eff} = 975 \pm 40$ K.

6. COMPARISON WITH STELLAR EVOLUTION THEORY

The absolute masses of VZ Cep have formal relative errors of 1% or better. The radius of the primary is similarly well determined, while that of the faint secondary is good to about 3.7%. These values along with the temperatures are compared here with stellar evolution models from the Yonsei-Yale series (Yi et al. 2001; Demarque et al. 2004). In Figure 7 the measurements are shown in the R vs. $T_{\rm eff}$ plane against evolutionary tracks computed for the measured masses and for solar metallicity ($Z = 0.01812$ in these models, indicated with solid lines). The shaded areas represent the uncertainty in the location of each track due to the measurement errors in the masses $M_{\rm A}$ and $M_{\rm B}$. While the primary track is in good agreement with our temperature determination for that star, the secondary track is too hot. Adjustment of the chemical composition of the models to $Z = 0.0280$ (corresponding to [Fe/H] $= +0.21$) provides the fit shown with the dotted lines. This fit is marginally consistent with our temperature error bars in the figure, but the agreement is misleading since the temperature *difference* is much better determined than the error bars appear to indicate. The best-fit age for this metallicity is 1.6 Gyr, and the corresponding isochrone is indicated with a dashed curve.

Figure 8 shows the measurements in the mass-radius diagram against the same set of models. The dashed line represents the same isochrone shown before, and the solid line is an isochrone for solar metallicity that provides the best fit, in this case for a slightly younger age of 1.4 Gyr. Both are seen to represent the measurements equally well.

These comparisons suggest that the models correctly predict the radii of the stars at the measured masses, but that the temperature of the secondary is underestimated by a significant amount. Tests with a different series of models by Pietrinferni et al. (2004) gave similar results.

7. DISCUSSION AND CONCLUSIONS

VZ Cep stands out among the F stars as one of the eclipsing binaries with the largest difference in mass between the components ($q = 0.7900$), which provides extra leverage for testing stellar evolution models. There are no less than five other systems with well determined properties (BW Aqr B, V1143 Cyg A, BP Vul B, V442 Cyg B, and AD Boo A; Andersen 1991; Lacy et al.
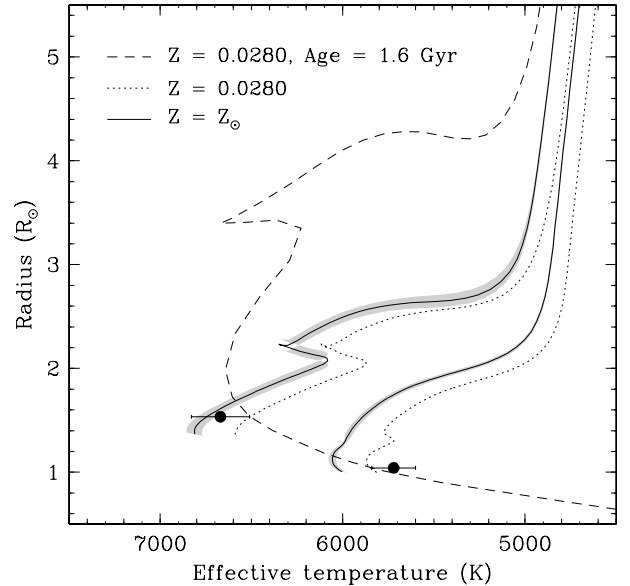

FIG. 7.— Stellar evolution models from the Yonsei-Yale series (Yi et al. 2001; Demarque et al. 2004) compared against the measurements for VZ Cep. Solid lines show evolutionary tracks for the measured masses and for solar metallicity ($Z = Z_\odot$), with the uncertainty in the location of the tracks represented by the shaded regions. Dotted lines correspond to mass tracks at a somewhat higher metallicity of $Z = 0.0280$ that seems to fit the observations better (see text). An isochrone for this metallicity and an age of 1.6 Gyr is shown with a dashed curve.
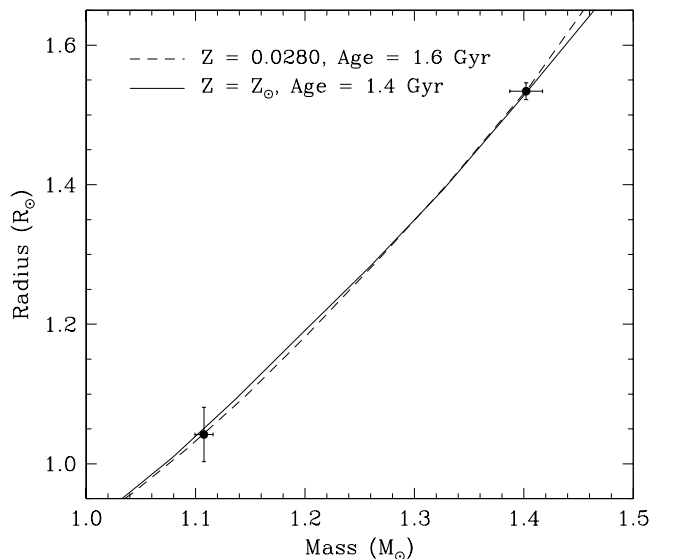
FIG. 8.— Isochrones from the Yonsei-Yale series (Yi et al. 2001; Demarque et al. 2004) compared with the measurements for VZ Cep in the mass-radius plane. The dashed line is the same isochrone shown in Figure 7 ($Z = 0.0280$), and a solar-metallicity isochrone is represented by the solid curve, for a slightly younger age that fits the observations best.

2003; Clausen et al. 2008) that have at least one component nearly identical in mass to the primary of VZ Cep (i.e., within 1%). However, these stars are all in very different evolutionary states so that their radii span a range of 33% and their effective temperatures differ by up to 360 K. They are therefore of little help in under-

standing the discrepancies with theory noted above for VZ Cep. Only one other well measured binary has one component with a mass similar to that of the secondary of VZ Cep, but that star (EK Cep B) is considered to be in the pre-main sequence stage (Popper 1987).

Figure 7 highlights the main disagreement between the models and the measurements for VZ Cep, which is that the temperature difference predicted from theory for the measured masses and surface gravities is much smaller than all of our estimates. Solar metallicity models, which appear to fit the properties of the primary well, indicate $\Delta T_{\rm eff} = 710$ K, and this is reduced further to 660 K when considering the higher metallicity of $Z = 0.0280$. The uncertainty in these determinations is difficult to quantify, but a useful measure may be obtained by propagating the uncertainty in the measured masses, which results in ± 50 K. Uncertainties from physical inputs to the models are unlikely to add much to this due to the differential nature of the comparison. In this paper we have made three empirical determinations of $\Delta T_{\rm eff}$, as follows: 1) $\Delta T_{\rm eff} = 970 \pm 35$ K, based on the $J_{\rm B}$ value from our light-curve analysis along with the visual flux scale of Popper (1980) and our spectroscopic brightness ratio (used as an external constraint); 2) $\Delta T_{\rm eff} = 975 \pm 40$ K, from photometric deconvolution based on the measured Strömgren indices and the spectroscopic brightness ratio (§ 5), along with the color/temperature calibrations of Holmberg et al. (2007); 3) $\Delta T_{\rm eff} = 940$ K, directly from a primary temperature estimate based on spectroscopy (§ 3) and an assumed temperature for the secondary similar to estimates for that star from the other two methods. While these three determinations are not completely independent, their consistency despite the widely different ingredients reinforces our conclusion that the model $\Delta T_{\rm eff}$ is at least $\sim$250 K too small.

Stellar evolution models have been shown previously to overestimate the effective temperatures of low-mass stars in eclipsing binaries by up to $\sim$200 K (e.g., Torres & Ribas 2002; Ribas 2003). The study of V1061 Cyg by Torres et al. (2006) suggested that the problem is not confined to M dwarfs, but extends up to masses almost as large as that of the Sun (0.93 $M_\odot$ in the case of V1061 Cyg B). At the same time, the radii of these stars appear too large compared to theory, and both discrepancies are generally attributed to the effects of stellar activity in these short-period, tidally synchronized and rapidly rotating systems.

There is little doubt that the VZ Cep system is active, judging by its strong X-ray emission as recorded by ROSAT (Voges et al. 1999). We estimate its X-ray luminosity to be $\log L_{\rm X} = 30.61 \pm 0.12$ (where $L_{\rm X}$ is in cgs units), and $\log L_{\rm X}/L_{\rm bol} = -3.70 \pm 0.13$.[5] The mass of VZ Cep B is slightly larger than that of the Sun, but it still has a thin convective envelope representing about 1.3% of the total mass, which suggests that star may in fact be responsible for most of the X-ray emission given that the primary has no convective envelope. Another indication is given by the Rossby numbers of the stars (ratio R_0 between the convective turnover time and the rotational period). For the primary we estimate $\log R_0 > 2.1$,

which according to Hall (1994, Fig. 6) clearly places it among the inactive stars. The secondary, on the other hand, has $\log R_0 = -1.3$. Stars in this regime tend to be very active and have photometric variability due to spots with amplitudes as large as $\sim$0.4 mag. Detection of this expected variability is difficult in VZ Cep because of the faintness of the secondary. Nevertheless, we examined the nightly residuals from our adopted solution near the primary minimum, where the contrast is more favorable, and we see only occasional systematic deviations on one or two nights. However, similar deviations are seen at the secondary eclipse, and also outside of eclipse, which leads us to believe these are residual instrumental errors rather than real changes in the light level caused by spottedness on the secondary (see § 4).

If we consider the properties of the primary of VZ Cep to be relatively well described by theory for a metallicity near solar, then the secondary shows a temperature difference compared to models in the same direction as mentioned above for other active stars (i.e., lower than predicted). However, we see no indication that its radius is larger than predicted (Figure 8), which we would have expected not only from the evidence displayed by other systems but also from recent theoretical studies of the effects of chromospheric activity (e.g., Mullan & MacDonald 2001; Chabrier et al. 2007).

As described in previous sections, we have carried out a variety of tests to explore the possibility of systematic errors in our mass, radius, or temperature determinations, including a careful examination of biases in our velocity measurements, and sanity checks of our light-curve analysis with results from more sophisticated modeling programs. We were unable to demonstrate any significant errors that would explain the discrepancies in the preceding paragraph. For example, matching the model $\Delta T_{\rm eff}$ with the $\Delta T_{\rm eff}$ measured from the light curve would require a change in the mass ratio to $q \approx 0.71$, much lower than allowed by the spectroscopy, regardless of the choice of cross-correlation templates (see § 3). Conversely, deriving a smaller temperature difference from the light curve to match the models would require an increase in $J_{\rm B}$ to values that are unrealistic and would bring strong disagreement with the light ratio from spectroscopy. Additionally, this would leave the other two empirical estimates of $\Delta T_{\rm eff}$ unchanged, and a discrepancy would remain. As indicated earlier, we see no evidence for third light at a level that would make much difference. The adjustments required in each of the quantities mentioned above, and others we experimented with, are so large compared to the uncertainties that a combination of effects is unlikely to resolve the issue either.

At the suggestion of the referee, we show in Figure 9 a comparison with an alternate set of models by Baraffe et al. (1998), which allows us to explore the effect of differences in the mixing length parameter $\alpha_{\rm ML}$. Previous studies of the radius and temperature discrepancies for active low-mass stars have indicated that a value of $\alpha_{\rm ML}$ lower than appropriate for the Sun, representing a reduced overall convective efficiency, provides a much better match to the observations of these objects. Consequently, we show a solar-metallicity evolutionary track for a solar-like mixing length parameter for the radiative primary ($\alpha_{\rm ML} = 1.9$ in these models), and tracks for three values of the mixing length parameter for the

---

[5] By comparison, $\log L_{\rm X}$ for the Sun ranges between 26.4 and 27.7 during the activity cycle (Peres et al. 2000), and $\log L_{\rm X}/L_{\rm bol}$ ranges between -7.2 and -5.9.
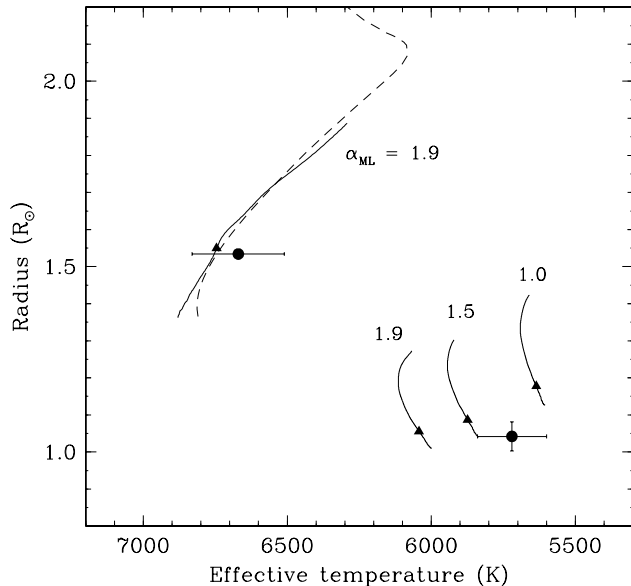
FIG. 9.— Radius and effective temperature of VZ Cep compared against evolutionary tracks for solar metallicity by Baraffe et al. (1998), for the exact masses we measure (solid lines). A single track is shown for the primary star, for a mixing length parameter $\alpha_{ML} = 1.9$ appropriate for the Sun. The dashed line represents the same solar-metallicity Yonsei-Yale track shown in Figure 7. Three Baraffe et al. (1998) models are shown for the secondary, for different values of α_{ML}, as labeled. For reference, the triangles on the solid curves correspond to an age of 1.4 Gyr, which was found in Figure 8 to provide a good match in the mass-radius plane using solar-metallicity models from the Yonsei-Yale series.

secondary star ($\alpha_{ML} = 1.9$, 1.5, and 1.0), which, as mentioned earlier, we believe to be the more active member of the system. For reference, triangles on each track mark the age of 1.4 Gyr, which we found in Figure 7 to provide the best match for $Z = Z_\odot$ using the Yonsei-Yale models. The Baraffe et al. (1998) model for the primary is seen to be similar to the corresponding solar-metallicity Yonsei-Yale model (dashed line, reproduced from Figure 7). A reduction of the mixing length parameter for the secondary star leads to the expected systematic decrease in effective temperature, and an increase in radius. A secondary model with α_{ML} between 1.0 and 1.5, when paired with the standard $\alpha_{ML} = 1.9$ model for the primary, would appear to give approximately the correct temperature difference for the system. However, the measured radius of VZ Cep B is somewhat smaller than predicted, in agreement with our earlier conclusion that this star appears normal in size (compared to standard models).

The 13% difference between our measured $v \sin i$ for the primary and the predicted synchronous velocity is somewhat puzzling, and is significant at the 2.5-σ confidence level. We do not believe errors in the spectroscopic measurements are to blame since all 39 of our individual spectra consistently give values smaller than predicted. A reduction in the predicted value could be accomplished with an increase in k, but it would have to be much larger than allowed by our photometric solutions, and would once again bring disagreement between the photometric and spectroscopic light ratios.

At the moment we are unable to offer an explanation for the differences noted above, and based on the tests just described we are inclined to believe that the measurements are accurate and that the system is affected in some way that the models do not account for, most likely having to do with chromospheric activity. It would also appear that our understanding of the effects of chromospheric activity (reduced convective efficiency, spot coverage) on the global properties of stars is still incomplete, since we see here only the effect on the temperature predicted by recent models that account for these phenomena (Chabrier et al. 2007), but not the effect on the radius. VZ Cep thus presents a challenge to theory. Further progress in understanding these differences may be made by obtaining complete light curves in multiple passbands, which would give a better handle on the temperature issue. Higher signal-to-noise ratio spectroscopy would also help in refining the $v \sin i$ measurements for the primary and secondary, in constraining the abundance, and perhaps also in providing a more direct determination of the effective temperatures and revealing whether Ca II emission is present.

REFERENCES

Agerer, F., & Huebscher, J. 1995, IBVS, No. 4222
Alonso, A., Arribas, S., & Martínez-Roger, C. 1996, A&A, 313, 873
Andersen, J. 1991, A&A Rev., 3, 91
Baraffe, I., Chabrier, G., Allard, F., & Hauschildt, P. H. 1998, A&A, 337, 403
Canon, A. J. 1934, Bull. Harvard Obs., 897, 12
Chabrier, G., Gallardo, J., & Baraffe, I. 2007, A&A, 472, L17
Claret, A. 1998, A&AS, 131, 395
Claret, A. 1998, A&A, 363, 1081
Claret, A. 2008, A&A, 482, 259
Clausen, J. V., Helt, B. E., & Olsen, E. H. 1999, in Theory and Tests of Convection in Stellar Structure, ASP Conf. Ser. 173, ed. A. Giménez, E. F. Guinan, & B. Montesinos (San Francisco: ASP), 321

Clausen, J. V., Torres, G., Bruntt, H., Andersen, J., Nordström, B., Stefanik R. P., Latham, D. W., & Southworth, J. 2008, A&A, 487, 1095
Crawford, D. L. 1975, AJ, 80, 955
Demarque, P., Woo, J.-H., Kim, Y.-C., & Yi, S. K. 2004, ApJS, 155, 667
Diethlem, R. 2006, IBVS, No. 5713
Etzel, P. B. 1981, Photometric and Spectroscopic Binary Systems (Dordrecht: Reidel), 65
Gengler, G. T., Blasko, S., & Schneller, H. 1928, AN, 233, 39
Gray, D. F. 1992, The Observation and Analysis of Stellar Photospheres, 2nd Edition (Cambridge: Cambridge Univ. Press)
Griffin, R. E. M., David, M., & Verschueren, W. 2000, A&AS, 147, 299

Hall, D. S. 1994, Mem. R. Astr. Soc., 65, 73

Holmberg, J., Nordström, B., & Andersen, J. 2007, A&A, 475, 519

Kim, C.-H., Lee, C.-U., Yoon, Y.-N., Park, S.-S., Kim, D.-H., Cha, S.-M., & Won, Y.-H. 2006, IBVS, No. 5694

Lacy, C. H., Freuh, M. L., & Turner, A. E. 1987, AJ, 94, 1035

Lacy, C. H. 1992, AJ, 104, 801

Lacy, C. H. S. 2002a, AJ, 124, 1162

Lacy, C. H. S. 2002b, IBVS, No. 5357

Lacy, C. H. S., Torres, G., Claret, A., & Sabby, J. A. 2003, AJ, 126, 1905

Lacy, C. H. S., Straughn, A., & Denger F. 2002, IBVS, No. 5251

Lacy, C. H. S., Torres, G., & Claret, A. 2008, AJ, 135, 1757

Lacy, C. H. S., Torres, G., Claret, A., & Vaz, L. P. R. 2005, AJ, 130, 2838

Latham, D. W. 1992, in IAU Coll. 135, Complementary Approaches to Double and Multiple Star Research, ASP Conf. Ser. 32, eds. H. A. McAlister & W. I. Hartkopf (San Francisco: ASP), 110

Latham, D. W., Stefanik, R. P., Torres, G., Davis, R. J., Mazeh, T., Carney, B. W., Laird, J. B., & Morse, J. A. 2002, AJ, 124, 1144

Mullan, D. J., & MacDonald, J. 2001, ApJ, 559, 353

Nelson, R. H. 2001, IBVS, No. 5040

Nelson, R. H. 2007, IBVS, No. 5760

Nordlund, Å, & Vaz, L. P. R. 1990, A&A, 228, 231

Nordström, B., Latham, D. W., Morse, J. A., Milone, A. A. E., Kurucz, R. L., Andersen, J., & Stefanik, R. P. 1994, A&A, 287, 338

Olsen, E. H. 1984, A&AS, 57, 443

Peres, G., Orlando, S., Reale, F., Rosner, R., & Hudson, H. 2000, ApJ, 528, 537

Perry, C. L., & Johnston, L. 1982, ApJS, 50, 451

Perryman, M. A. C., et al. 1997, The *Hipparcos* and *Tycho* Catalogues (ESA SP-1200; Noordwjik: ESA)

Pietrinferni, A., Cassisi, S., Salaris, M., & Castelli, F. 2004, ApJ, 612, 168

Popper, D. M. 1980, ARA&A, 18, 115

Popper, D. M. 1987, ApJ, 313, L81

Popper, D. M. 1996, ApJS, 106, 133

Popper, D. M. 1997, AJ, 114, 1195

Popper, D. M. 2000, AJ, 119, 2391

Popper, D. M., & Etzel, P. B. 1981, AJ, 86, 102

Ribas, I. 2006, Ap&SS, 304, 89

Ribas, I. 2003, A&A, 398, 239

Rössiger, S. 1978, IBVS, No. 1474

Sarounova, L., & Wolf, M. 2005, IBVS, No. 5594

Southworth, J. 2008, MNRAS, 386, 1644

Southworth, J., Bruntt, H., & Buzasi, D. L. 2007, A&A, 467, 1215

Torres, G., Andersen, J., Nordström, B., & Latham, D. W. 2000, AJ, 119, 1942

Torres, G., Neuhäuser, R., & Guenther, E. W. 2002, AJ, 123, 1701

Torres, G., Stefanik, R. P., Andersen, J., Nordström, B., Latham, D. W., & Clausen, J. V. 1997, AJ, 114, 2764

Torres, G., Lacy, C. H. S., Marschall, L. A., Sheets, H. A., & Mader, J. A. 2006, ApJ, 640, 1018

Torres, G., & Ribas, I. 2002, ApJ, 567, 1140

van Hamme, W. 1993, AJ, 106, 2096

van Hamme, W., & Wilson, R. E. 2007, ApJ, 661, 1129

Vaz, L. P. R. 1984, Ph.D. Thesis, Copenhagen University (unpublished)

Vaz, L. P. R. 1986, Rev. Mexicana Astron. Astrofis., 12, 177

Vaz, L. P. R., & Nordlund, Å 1985, A&A, 147, 281

Voges, W. et al. 1999, A&A, 349, 389

Wilson, R. E., & Devinney, E. J. 1971, ApJ, 166, 605

Wilson, R. E. 1979, ApJ, 234, 1054

Wilson, R. E. 1990, ApJ, 356, 613

Wilson, R. E. 1993, in New Fronteers in Binary Star Research, ASP Conf. Ser. 38, ed. K.-C. Leung & I.-S. Nha (San Francisco: ASP), 91

Wood, D. B. 1972, A Computer Program for Modeling Non-Spherical Eclipsing Binary Star Systems, Goddard Space Flight Center, Greenbelt, Maryland

Yi, S. K., Demarque, P., Kim, Y.-C., Lee, Y.-W., Ree, C. H., Lejeune, T., & Barnes, S. 2001, ApJS, 136, 417

Zucker, S., & Mazeh, T. 1994, ApJ, 420, 806

TABLE 1
Published measurements of the times of eclipse for VZ Cep.

HJD (2,400,000+)	Type[a]	Uncertainty (days)	$(O-C)$ (days)	Source
49567.42210.....	1	0.0003	+0.00067	1
51608.72370.....	1	0.0003	−0.00023	2
52038.87680.....	2	0.0005	−0.00012	3
52044.79410.....	2	0.0005	+0.00036	3
52051.89410.....	2	0.0005	+0.00018	3
52054.85215.....	1	0.00011	+0.00008	3
52073.78570.....	1	0.0002	−0.00019	3
52076.74440.....	2	0.0003	−0.00016	3
52079.70300.....	1	0.0003	+0.00029	3
52080.88604.....	1	0.00019	−0.00003	3
52093.90270.....	1	0.0005	−0.00038	3
52108.69630.....	2	0.0003	+0.00092	3
52111.65270.....	1	0.0006	−0.00083	3
52112.83709.....	1	0.00014	+0.00019	3
52114.61500.....	2	0.0006	+0.00280	3
52154.84470.....	2	0.0004	−0.00187	3
52159.58000.....	2	0.0010	−0.00002	3
52166.67970.....	2	0.0003	−0.00051	3
52179.69710.....	2	0.0003	−0.00011	3
52233.54070.....	1	0.0004	+0.00070	3
52277.32429.....	1	0.00007	−0.00017	4
52463.70530.....	2	0.0003	+0.00079	5
52464.88810.....	2	0.0003	+0.00022	5
52482.63870.....	2	0.0005	+0.00037	5
52518.73064.....	1	0.00019	−0.00003	5
53366.01950.....	1	0.0002	+0.00037	6
53658.30900.....	1	0.0006	−0.00098	7
54009.76910.....	1	0.0001	+0.00008	8

Note. — References: 1. Agerer & Huebscher (1995); 2. Nelson (2001); 3. Lacy et al. (2002); 4. Sarounova & Wolf (2005); 5. Lacy (2002b); 6. Kim et al. (2006); 7. Diethlem (2006); 8. Nelson (2007).
[a] Type: 1 = primary eclipse; 2 = secondary eclipse.

TABLE 2
RADIAL VELOCITY MEASUREMENTS OF VZ CEP.

HJD (2,400,000+)	RV_A (km s^{-1})	RV_B (km s^{-1})	$(O-C)_A$ (km s^{-1})	$(O-C)_B$ (km s^{-1})	Orbital phase
52661.5709	+106.35	−149.88	+1.69	+2.71	0.707
52808.9615	−127.46	+139.25	+1.12	−3.40	0.259
52828.9269	−96.88	+102.39	+0.15	−0.32	0.131
52834.9798	−127.64	+147.21	+1.10	+4.36	0.246
52885.8243	−126.22	+134.87	−0.81	−3.76	0.212
52894.8309	+96.39	−136.82	−0.31	+5.69	0.823
52924.7873	−100.02	+112.30	+0.34	+5.38	0.138
52951.7261	+57.66	−102.06	−0.97	−7.73	0.902
52958.6957	+105.49	−155.58	+0.59	−2.69	0.792
53013.5806	−114.11	+129.47	+0.78	+4.16	0.172
53182.9448	−125.76	+138.43	−1.35	+1.06	0.293
53185.9637	+88.37	−131.20	−0.31	+1.16	0.845
53186.9164	+88.42	−133.24	+2.37	−4.21	0.650
53189.9839	−129.03	+137.70	−0.41	−4.99	0.242
53191.8776	+89.70	−128.04	0.00	+5.61	0.842
53192.9211	+106.23	−154.75	−1.14	+1.27	0.724
53215.9246	−112.11	+119.86	−0.73	−1.02	0.163
53218.8991	+94.48	−137.57	−2.02	+4.69	0.677
53271.6999	−122.28	+137.26	+1.64	+0.51	0.296
53272.7658	−122.11	+134.75	−0.01	+0.31	0.197
53274.6998	+94.19	−144.23	+0.17	−5.11	0.831
53275.7597	+104.75	−162.66	−2.93	−6.25	0.727
53281.7191	+107.50	−158.17	−1.13	−0.56	0.763
53282.8175	+100.85	−144.52	+0.05	+3.18	0.691
53301.7530	+100.90	−147.17	−0.28	+1.01	0.692
53333.7365	+106.56	−150.44	−0.27	+4.89	0.720
53335.6589	−109.05	+117.57	−0.46	+0.23	0.344
53336.6417	−116.21	+124.74	−0.51	−1.60	0.175
53339.6764	+108.41	−157.55	−0.30	+0.16	0.739
53630.7663	+106.36	−156.85	−1.07	−0.75	0.724
53636.7401	+108.74	−160.82	+0.93	−4.24	0.773
53690.6534	−112.94	+127.71	+0.49	+4.24	0.332
53691.7072	−127.60	+134.58	−0.62	−6.04	0.222
54042.6132	+111.73	−160.65	+2.80	−2.66	0.755
54043.7068	+98.06	−145.42	+0.68	−2.05	0.679
54074.5790	+106.66	−154.30	−1.60	+2.85	0.768
54103.5713	−127.62	+139.12	+0.44	−2.87	0.268
54279.9427	−121.65	+138.43	−1.19	+6.07	0.310
54282.8950	+105.11	−148.54	+3.09	+0.71	0.805

NOTE. — These velocities include corrections for systematics (see text).

TABLE 3
Spectroscopic orbital solution for VZ Cep.

Parameter	Value
Adjusted quantities	
P (days)[a]	1.18336377
$T_{\rm I}$ (HJD$-$2,400,000)[a]	52,277.32446
$K_{\rm A}$ (km s^{-1})	118.88 ± 0.22
$K_{\rm B}$ (km s^{-1})	150.48 ± 0.67
γ (km s^{-1})	-9.90 ± 0.21
ΔRV (km s^{-1})[b]	-2.31 ± 0.65
Derived quantities	
$M_{\rm A} \sin^3 i$ (M$_\odot$)	1.339 ± 0.013
$M_{\rm B} \sin^3 i$ (M$_\odot$)	1.0577 ± 0.0064
$q \equiv M_{\rm B}/M_{\rm A}$	0.7900 ± 0.0038
$a_{\rm A} \sin i$ (10^6 km)	1.9345 ± 0.0036
$a_{\rm B} \sin i$ (10^6 km)	2.4487 ± 0.0109
$a \sin i$ (R$_\odot$)	6.298 ± 0.016
Other quantities pertaining to the fit	
$N_{\rm obs}$	39
Time span (days)	1621.3
$\sigma_{\rm A}$ (km s^{-1})	1.27
$\sigma_{\rm B}$ (km s^{-1})	3.82

[a] Ephemeris adopted from § 2. [b] Velocity offset in the sense ⟨primary−secondary⟩ (see text).

TABLE 4
Differential V-band magnitudes of VZ Cep.

HJD$-$2,440,000	ΔV	Orbital phase
51973.95823	0.129	0.64077
51973.95926	0.115	0.64164
51973.96028	0.123	0.64250
51973.96130	0.126	0.64336
51973.96233	0.126	0.64423

Note. — Table 4 is available in its entirety in the electronic edition of the *Astronomical Journal*. A portion is shown here for guidance regarding its form and contents.

TABLE 5
Photometric orbital solutions for VZ Cep.

Parameter	Unconstrained fit	Constrained fit
$J_{\rm B}$	0.495 ± 0.010	0.4920 ± 0.0013
$k \equiv r_{\rm B}/r_{\rm A}$	0.717 ± 0.041	0.680 ± 0.030
$r_{\rm A} + r_{\rm B}$	0.4077 ± 0.0043	0.4028 ± 0.0077
$r_{\rm A}$	0.2374 ± 0.0033	0.2398 ± 0.0017
$r_{\rm B}$	0.1703 ± 0.0073	0.1630 ± 0.0061
$u_{\rm A}$	0.499 ± 0.075	0.420 ± 0.076
$u_{\rm B}$	0.581 ± 0.059	0.500 ± 0.076
i (deg)	79.47 ± 0.44	79.97 ± 0.45
$L_{\rm A}(V)$[a]	0.802 ± 0.022	0.820 ± 0.014
$(L_{\rm B}/L_{\rm A})_V$	0.246 ± 0.033	0.220 ± 0.020[b]
σ_V (mmag)	7.4400	7.4365
$N_{\rm obs}$	5473	5473

[a] Fractional luminosity of the primary. [b] Adopted as a constraint from spectroscopy (see text).

TABLE 6
PHYSICAL PROPERTIES OF VZ CEP.

Parameter	Primary		Secondary
Mass $(M_\odot)$	1.402 ± 0.015		1.1077 ± 0.0083
Radius $(R_\odot)$	1.534 ± 0.012		1.042 ± 0.039
$\log g$ (cgs)	4.2130 ± 0.0080		4.446 ± 0.033
Temperature (K)	6670 ± 160		5720 ± 120
$\log L$ $(L_\odot)$	0.634 ± 0.041		0.026 ± 0.050
$v \sin i$ $(\mathrm{km\,s^{-1}})^a$	57 ± 3		50 ± 10
$v_{\mathrm{sync}} \sin i$ $(\mathrm{km\,s^{-1}})^b$.	64.6 ± 0.5		43.9 ± 1.6
a $(R_\odot)$		6.396 ± 0.019	
Distance (pc)		215 ± 10	
M_{bol} (mag)	3.18 ± 0.10		4.68 ± 0.12
M_V (mag)	3.16 ± 0.11		4.77 ± 0.12

[a] Value measured spectroscopically. [b] Value predicted assuming synchronous rotation.